



Düzce University Journal of Science & Technology

Research Article



Sustainable Dye-Sensitized Solar Cells Enhanced with CdS and Natural *Peltophorum pterocarpum* Dye for Dual Energy and Low-Light Sensing: The Synergistic Role of ZnO Nanorods and Natural Dyes

 Mücella ÖZBAY KARAKUŞ^{a,*}

^a Department of Computer Engineering, Faculty of Engineering and Architecture, İzmir Bakırçay University, İzmir, TURKEY

* Corresponding author's e-mail address: mucella.ozbaykarakus@bakircay.edu.tr

DOI: 10.29130/dubited.1668896

ABSTRACT

This study presents a novel and sustainable approach to dye-sensitized solar cell (DSSC) design by integrating a natural dye extracted from *Peltophorum pterocarpum* with CdS co-sensitization and ZnO nanorod-modified TiO₂ photoelectrodes. The fabricated DSSCs were enhanced through the integration of ZnO nanorods on TiO₂ photoelectrodes and further modified with CdS co-sensitization to boost their photovoltaic and photodetection capabilities. The devices were evaluated under a broad range of light intensities (100 to 0.01 mW/cm²), revealing dual functionality: efficient photovoltaic operation under standard illumination and superior sensitivity under ultra-low light. Under standard illumination, the highest efficiency (8.15%) was achieved with N719 dye and ZnO/TiO₂ electrodes. However, the *P. pterocarpum*-based cells also exhibited competitive performance, reaching 6.92% with CdS and ZnO enhancement. Remarkably, under ultra-low light (0.01 mW/cm²), the natural dye-based DSSCs demonstrated power conversion efficiencies exceeding 18%, rivaling commercial dye systems. These results highlight the synergistic role of ZnO nanorods and CdS in enhancing charge transport and light absorption, while also showcasing the viability of natural dyes for eco-friendly, low-cost optoelectronic applications. This study is among the first to demonstrate the synergistic integration of *P. pterocarpum* natural dye, CdS co-sensitization, and ZnO nanorods in DSSCs and in this research, sustainable natural dye utilization with structural nanomaterial engineering is uniquely bridged to develop DSSCs capable of dual functionality under both standard and ultra-low light conditions.

Keywords: Dye-sensitized solar cell (DSSC), *Peltophorum pterocarpum* natural dye, CdS co-sensitization, low-light photodetection, ZnO nanorods with TiO₂ photo electrode

CdS katkısıyla Desteklenmiş Doğal *Peltophorum pterocarpum* ile Sürdürülebilir Boya Duyarlı Güneş Hücreleri: ZnO Nanorodların ve Doğal Boyaların Enerji Üretimi ve Düşük Işık Algılamadaki Sinerjik Rolü

ÖZ

Bu çalışma, *Peltophorum pterocarpum* bitkisinden elde edilen doğal bir boyanın CdS eş-duyarlılaştırması ve ZnO nanorod ile modifiye edilmiş TiO₂ fotoelektrotlarla entegre edilmesiyle, boya duyarlı güneş hücresi (DSSC) tasarımına yenilikçi ve sürdürülebilir bir yaklaşım sunmaktadır. Üretilen DSSC'ler, TiO₂ fotoelektrotlara entegre edilen ZnO nanorodlar ve CdS eş-duyarlılaştırması sayesinde hem fotovoltajik hem de fotodetektör performansları açısından geliştirilmiştir. Cihazlar, 100 ila 0.01 mW/cm² arasında geniş bir ışık yoğunluğu aralığında değerlendirilmiş ve bu sayede hem standart aydınlatma koşullarında verimli enerji üretimi hem de ultra düşük ışık seviyelerinde üstün algılama hassasiyeti olmak üzere çift işlevlilik ortaya konmuştur.

Standart aydınlatma koşullarında en yüksek verim (%8.15), N719 boyası ve ZnO/TiO₂ elektrotlar ile elde edilmiştir. Ancak *P. pterocarpum* bazlı hücreler de CdS ve ZnO katkısı ile %6,92'ye ulaşarak rekabetçi bir performans sergilemiştir. Dikkat çekici şekilde, ultra düşük ışık koşullarında (0.01 mW/cm²) doğal boya bazlı DSSC'ler %18'in üzerinde güç dönüşüm verimliliği sağlayarak ticari boyalara rakip olmuştur. Bu sonuçlar, ZnO nanorodlar ve CdS'nin yük taşıma ve ışık soğurma süreçlerini artırmadaki sinerjik rolünü vurgularken, doğal boyaların çevre dostu ve düşük maliyetli optoelektronik uygulamalardaki potansiyelini de gözler önüne sermektedir.

Bu çalışma, *P. pterocarpum* doğal boyasının, CdS eş-duyarlılaştırması ve ZnO nanorodlarla sinerjik entegrasyonunu DSSC yapılarında ilk kez sistematik olarak ortaya koymakta ve sürdürülebilir doğal boya kullanımı ile nanoyapısal mühendislik arasındaki köprüyü kurarak hem standart hem de ultra düşük ışık koşullarında çift işlevli çalışabilen DSSC'lerin geliştirilmesine olanak tanımaktadır.

Anahtar Kelimeler: *Boya duyarlı güneş hücresi (DSSC), Peltophorum pterocarpum esaslı doğal boya, CdS yardımcı duyarlılaştırıcı, düşük ışık algılama, ZnO nanorod ilaveli TiO₂ foto elektrot*

I. INTRODUCTION

Dye-sensitized solar cells (DSSCs) are a third-generation photovoltaic technology that converts solar energy into electrical energy and has gained significant attention due to the increasing global demand for clean and renewable energy sources [1, 2]. The environmental drawbacks of fossil fuels—such as the release of carbon dioxide, sulfur dioxide, and carbon monoxide, which contribute to global warming and to air pollution—and their limited availability have further emphasized the need for alternative energy solutions [1, 3]. In this regard, solar cells offer a low-cost and eco-friendly alternative. Although silicon-based p–n junction solar cells can achieve high efficiencies [4], their fabrication remains costly, encouraging the exploration of more affordable and efficient photovoltaic designs. However, silicon-based solar cells often experience significant efficiency losses under non-direct illumination, such as in indoor environments, cloudy weather, or rainy conditions, which limits their practical usability in low-light or diffused light scenarios.

In 1991, Michael Grätzel and colleagues introduced a DSSC using TiO₂ and a ruthenium-based dye, achieving a power conversion efficiency of up to 13% [5]. DSSCs present several advantages, including low production cost, ease of fabrication, large-scale manufacturability, environmental compatibility, and acceptable efficiency, making them attractive candidates for practical applications [1, 3, 6]. However, the most widely used dyes in DSSCs, such as N719 and N3, are ruthenium-based, which limits their long-term sustainability due to their high cost and limited availability [10–13]. To address this issue, researchers have explored natural, abundantly available dyes as alternative sensitizers for TiO₂-based photoanodes in DSSCs [14]. Natural dyes offer several advantages, including biodegradability, low toxicity, cost-effectiveness, and ease of extraction. However, their performance is often limited by low stability and light absorption efficiency. Therefore, systematic studies are needed to improve the efficiency and durability of natural dye-based DSSCs.

DSSCs typically consist of a photoanode made from a transparent conductive oxide glass substrate coated with a porous nanocrystalline wide-bandgap semiconductor (e.g., TiO₂ or ZnO), a counter electrode (commonly platinum or graphite), and a redox electrolyte responsible for regenerating the dye

and facilitating electron transfer within the cell [7–9]. Recent studies have shown that incorporating semiconducting materials such as CdS and P3HT into DSSCs can enhance light absorption and improve charge transfer efficiency [15, 16]. For instance, CdS–P3HT hybrid structures have achieved conversion efficiencies of up to 4.1% [17]. Research efforts are ongoing to optimize CdS-based DSSCs by improving the charge transport properties of the nanomaterials used [18, 19].

Moreover, natural dye extracts derived from the *Peltophorum pterocarpum* plant offer an eco-friendly and low-cost alternative for DSSCs. A previous study reported a power conversion efficiency of 6.07% using this natural dye [19]. When combined with CdS as a co-sensitizer, further efficiency enhancement may be achieved due to improved spectral coverage and charge injection dynamics. CdS has also been recognized as one of the earliest materials used in thin-film PV technology and continues to be explored for DSSC applications [18].

ZnO nanostructures have attracted considerable attention in DSSC research due to their high electron mobility, ease of synthesis, and structural versatility [20, 21]. As a typical n-type semiconductor, ZnO can be fabricated into nanorods, nanoparticles, or nanotubes using various deposition techniques, including hydrothermal growth, chemical vapor deposition, and electrochemical methods [13, 22–24]. DSSCs fabricated with ZnO nanoparticles have shown the second-highest efficiencies after TiO₂-based systems. Furthermore, the processing and properties of ZnO nanostructures, as well as the wide variety of accessible morphologies through vapor deposition, hydrothermal, or solution growth methods, are well documented in the literature [25, 26]. ZnO exhibits higher electron mobility, making it a more desirable photoanode material for DSSCs. In principle, to enhance the power conversion efficiency of a DSSC, it is essential to obtain a photoanode with a high surface area and low electron recombination rate [20, 21]. While most natural dye applications in DSSCs have focused on TiO₂-based systems [27, 28], exploring the behavior of natural dyes in ZnO-based architectures is becoming increasingly important for boosting overall device efficiency [29].

This study aims to systematically evaluate the photovoltaic and photodetection performances of DSSCs fabricated using the natural *P. pterocarpum* dye, with and without CdS co-sensitization, on TiO₂ and ZnO NRs/TiO₂ photoanodes. The experimental approach presented in the study involves the hydrothermal growth of ZnO nanoparticles on TiO₂ films to be used as photoanodes in DSSCs. The increased specific surface area provided by the ZnO nanostructures is expected to enhance dye molecule adsorption and improve device performance. Accordingly, DSSCs based on TiO₂/ZnO nanorod structures were investigated in combination with a natural dye extracted from *Peltophorum pterocarpum*. The power conversion efficiency of the fabricated DSSCs was analyzed via J–V characterization.

Furthermore, it is known that conventional c-Si and heterojunction solar cells generate a photocurrent within a time frame ranging from a few to several hundred milliseconds. In contrast, DSSCs are known to produce photocurrent more slowly due to their reliance on electrochemical processes [30]. One of these processes is electron recombination, which limits DSSC performance and occurs when electrons injected from the excited dye into the mesoporous semiconductor or from the electrolyte into the dye recombine [31]. Therefore, the materials used in DSSC structures greatly influence critical photodetector parameters such as detection sensitivity and temporal response. In this context, the sensitizing dyes used in the photoanodes play a critical role in determining the electricity generation and overall performance of DSSCs.

To this end, this work explores DSSC structures not only as energy conversion devices, but also aims to develop an accessible and economical process for ultra-sensitive photodetectors with relatively fast response times under low-light conditions. A comparative study was conducted between DSSCs using the commercial N719 dye and those sensitized with ethanol-extracted *P. pterocarpum* dye. The impact of CdS co-sensitization on the natural dye adsorbed onto the TiO₂ photoanode was also assessed. The photovoltaic and photodetection performance of the devices was evaluated under a range of light intensities as 15, 8, 2, 1, 0.5, 0.2, 0.1, 0.05, and 0.01 mW/cm², and the results were compared against a high-quality commercial c-Si photodetector. Although ZnO nanostructures and CdS co-sensitization

have individually been studied in DSSC literature, their synergistic effect—particularly when used in combination with natural dyes—has received limited attention. This study fills that gap by systematically investigating the integrated influence of ZnO nanorods and CdS on the dual-mode performance of natural dye-based DSSCs.

II. MATERIALS & METHOD

In this study, six different configurations of dye-sensitized solar cells (DSSCs) were fabricated and characterized. As the natural dye, leaves of *Peltophorum pterocarpum* (commonly known as yellow poinciana) were collected, washed, and then left to dry in the shade at room temperature. Once dried, the leaves were ground into coarse powder. Approximately 25 grams of the powdered *P. pterocarpum* leaves were soaked in 100 mL of ethanol in a sealed container for 48 hours at room temperature in a dark environment to extract the dye. After the extraction period, the mixture was filtered using filter paper to obtain a clear solution, which was subsequently stored wrapped in aluminum foil to prevent exposure to light. Figure 1 presents the image of the *P. pterocarpum* flower along with the ethanol-extracted dye solution derived from its leaves.



Figure 1. The flower of *Peltophorum pterocarpum* (yellow poinciana) and the natural dye extract are prepared from its leaves using ethanol extraction.

To investigate the effect of CdS incorporation on the dye performance, additional DSSC structures were fabricated using *P. pterocarpum* dye with CdS additives. For comparison, a commercially available dye, N719, was also used in another series of DSSCs.

In photoelectrode fabrication, two different types were employed: a standard TiO₂ layer and a TiO₂ layer reinforced with ZnO nanoparticles. Fluorine-doped tin oxide (FTO)-coated glass substrates (7 Ω/cm²), commercially purchased, were first cleaned with detergent, rinsed with deionized water, and dried using nitrogen gas. TiO₂ paste (Ti-Nanoxide D/SP) was applied on the FTO substrate using the doctor blade technique to form a 5×5 mm² active area. The electrodes were then sintered gradually, reaching 450°C for 30 minutes [32].

For the standard TiO₂-based photoelectrodes, a 40 mM aqueous TiCl₄ solution was heated to 70°C, and the TiO₂ electrodes were treated in this solution for 30 minutes. Afterwards, the electrodes were rinsed with deionized water and ethanol, followed by a second sintering process at 450°C for 30 minutes. DSSCs using these electrodes were coded as “TiO₂”.

For ZnO nanoparticles-reinforced photoelectrodes, the same procedure was followed up to the initial sintering step. Then, ZnO nanoparticles were grown on the TiO₂ film via a hydrothermal method. Specifically, 2.195 g of zinc acetate dihydrate (Zn(CH₃COO)₂·2H₂O) and 0.6 mL monoethanolamine were mixed in 40 mL methanol and stirred for 5 hours. The solution was then spin-coated onto the surface and dried at 300°C for 3 minutes. Seed layer formation was completed by annealing at 600°C for 30 minutes. Next, 0.1 M zinc acetate dihydrate and 1 M hexamethylenetetramine were dissolved in 100 mL of water and stirred for 1 hour. The resulting solution was transferred to a Teflon-lined autoclave, and the samples were placed horizontally. A hydrothermal growth process was carried out at

90°C for 3 hours. After cooling to room temperature, the samples were thoroughly rinsed with water, dried with nitrogen, and annealed at 400°C for 30 minutes to complete the nanoparticles growth. DSSCs using these electrodes were labeled as “ZnO/TiO₂”.

After preparation, the photoelectrodes were cooled to approximately 50–60°C, then immersed in the ethanolic *P. pterocarpum* dye solution under dark conditions at room temperature for 18 hours. Subsequently, they were rinsed with ethanol and water and then dried. The first series of DSSCs fabricated using TiO₂ and ZnO/TiO₂ photoelectrodes were labeled as “Pp (TiO₂)” and “Pp (ZnO/TiO₂)”, respectively.

For the second series, CdS-modified dye was prepared by dispersing commercially purchased CdS-n powder in dimethyl sulfoxide (DMSO). This solution was spin-coated onto the surface of photoelectrodes previously sensitized with the *P. pterocarpum* dye, forming a porous CdS-n layer. The samples were then annealed at 170°C for 10 minutes in air. These DSSCs were labeled as “Pp-CdS (TiO₂)” and “Pp-CdS (ZnO/TiO₂)”.

For the third series (comparison group), the photoelectrodes were cooled to 50–60°C after sintering and immersed under dark conditions at room temperature for 18 hours in a 0.5 mM ethanolic solution of Ruthenizer 535-bisTBA (N719) dye, which was prepared with a 10:1 weight ratio of chenodeoxycholic acid as a co-adsorbent. After immersion, the electrodes were rinsed with water and ethanol, then dried. These DSSCs were coded as “N719 (TiO₂)” and “N719 (ZnO/TiO₂)”.

The counter electrodes, common to all DSSC structures, consisted of FTO glass coated with platinum and were sintered at 420°C for 15 minutes. The photoelectrodes and counter electrodes were assembled using a 60 µm thick thermoplastic sealing film (Meltonix 1170-60) to form a sandwich structure. A liquid electrolyte containing an iodide/triiodide redox couple was then injected into the cell gap. Platinum electrodes and Meltonix 1170-60 were obtained from Solaronix, while other chemicals were purchased from Merck. To ensure reproducibility and minimize experimental errors, three independent samples were prepared for each DSSC type.

To evaluate the properties of the fabricated DSSCs, the structural parameters were first analyzed in detail. Subsequently, a series of experiments were conducted to determine photovoltaic efficiency and photodetector functions. Current-voltage (I–V) measurements were performed using a Science Tech SLB-300A under an illumination intensity of 100 mW/cm² with an AM1.5 filter. Additionally, the electrical characteristics of the DSSCs were evaluated under various illumination intensities, assuming a specific spectral distribution. During testing, the temperature was kept constant at 298 K (25°C), and neutral density filters were used to adjust the light intensity to 15, 8, 2, 1, 0.5, 0.2, 0.1, 0.05, and 0.01 mW/cm². For each light intensity level, the performance parameters of the cells were carefully measured.

III. RESULTS & DISCUSSION

To evaluate the photovoltaic performance of dye-sensitized solar cells (DSSCs) utilizing *Peltophorum pterocarpum*-based natural dye and ZnO nanorod-decorated TiO₂ photoelectrodes, current–voltage (I–V) measurements were performed under AM1.5 illumination at an intensity of 100 mW/cm². The resulting I–V curves are presented in Figure 2. From these measurements, key photovoltaic parameters including open-circuit voltage (V_{OC}), short-circuit current density (J_{SC}), and the maximum power point (V_{mp} , J_{mp}) were extracted. Subsequently, the fill factor (FF) and energy conversion efficiency (η) were calculated using Equations (1) and (2), respectively. The data obtained for each DSSC configuration were thoroughly analyzed to understand the influence of different dye and photoelectrode combinations on device performance.

$$FF = \frac{V_{max} \times J_{max}}{V_{oc} \times J_{sc}} \quad (1)$$

$$\eta(\%) = \frac{V_{oc} \times J_{sc} \times FF}{P_{in}} \quad (2)$$

The current–voltage (I–V) curves presented in Figure 2 clearly demonstrate the impact of various photoelectrode architectures and dye sensitizers on the overall performance of the DSSCs. Among the tested configurations, the device utilizing N719 dye with ZnO nanorod-decorated TiO₂ photoelectrodes exhibited the highest power conversion efficiency (PCE) of 8.15%, indicating the synergistic effect of the commercial dye and the nanostructured electrode. The second-best performance (8.06%) was observed for the cell using N719 with a conventional TiO₂ electrode, confirming the superior sensitizing capability of N719 under standard illumination conditions.

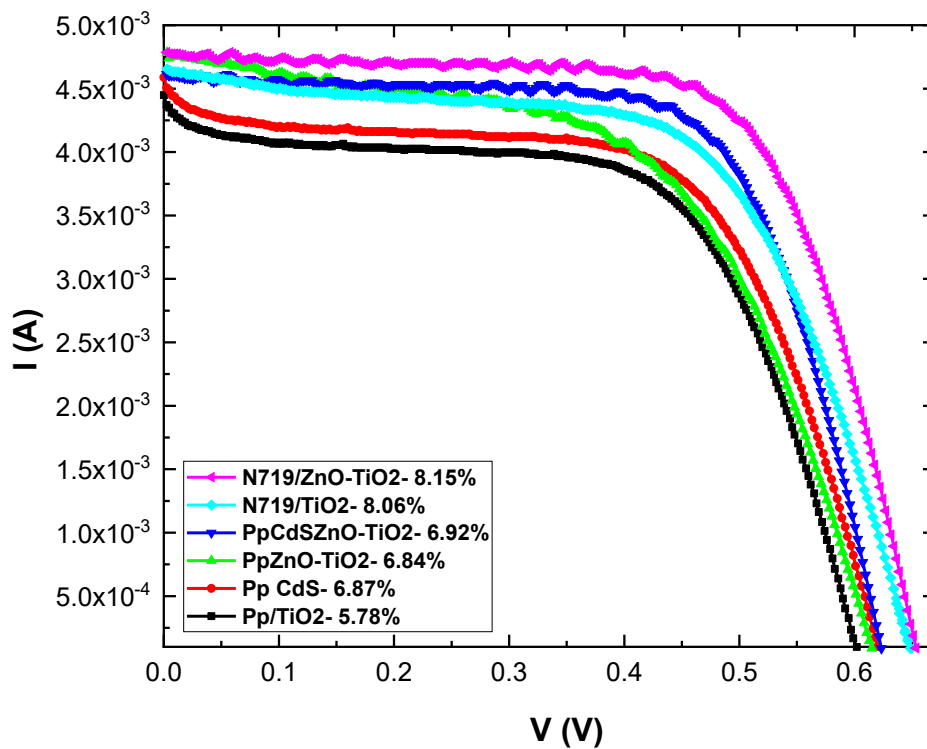


Figure 2. Current–voltage (I–V) characteristics of DSSCs fabricated with different configurations under 100 mW/cm² illumination intensity (AM 1.5 conditions). The inset shows a cross-sectional SEM image of ZnO nanorods (ZnO NRs) vertically grown on a TiO₂ layer deposited over an FTO substrate.

Additionally the devices incorporating ZnO nanorod-enhanced TiO₂ photoelectrodes exhibited higher short-circuit current density (J_{sc}) and open-circuit voltage (V_{oc}) compared to those using standard TiO₂ electrodes. This enhancement can be attributed to the increased surface area provided by the ZnO nanostructures, enabling greater dye loading and more efficient electron transport.

Notably, the DSSC fabricated with *Peltophorum pterocarpum* dye and CdS co-sensitization on ZnO-TiO₂ photoelectrodes achieved a commendable PCE of 6.92%, outperforming the same configuration without CdS (6.84%) and even the CdS-modified natural dye on TiO₂ alone (6.87%) while the device with only *P. pterocarpum* dye showed slightly lower value of 5.78%. The device using only *P. pterocarpum* dye on a standard TiO₂ photoelectrode which has the lowest recorded efficiency (5.78%), underscoring the beneficial effect of structural and material modifications. These results validate the potential of natural dyes, particularly when combined with nanostructured electrodes and co-sensitizers like CdS, to approach the performance levels of conventional DSSCs while maintaining eco-friendly

and cost-effective attributes. This suggests that both the ZnO nanostructures and CdS co-sensitization contribute to enhanced electron transport and light harvesting. On the other hand, the combination of *P. pterocarpum*-based natural dye with ZnO/TiO₂ electrodes highlights the viability of natural dyes in DSSC applications and underscores their potential in the development of eco-friendly photovoltaic technologies.

The reference c-Si device yielded a comparatively modest efficiency of 3.80%. These results suggest that while natural dye-based DSSCs may not surpass commercial dyes under full sunlight, they still offer competitive performance at reduced cost and environmental impact.

The performance of DSSC structures under low light intensity conditions is of critical importance for their potential application in photodetectors. The experiments were conducted under controlled laboratory conditions and extended to the lowest measurable illumination levels to evaluate the sensitivity and responsiveness of the fabricated DSSCs. For this purpose, the performance of the cells was monitored under varying light intensities over time, providing insight into their stability and adaptability under different illumination scenarios. During all measurements, the temperature was kept constant at 298 K (25°C), and neutral density filters were employed to modulate the incident light intensity in a sequential manner: 15, 8, 2, 1, 0.5, 0.2, 0.1, 0.05, and 0.01 mW/cm². Notably, all devices were able to produce a measurable output even at ultra-low light intensities such as 0.01 mW/cm², clearly demonstrating their capability to function in dim environments and highlighting their high detection sensitivity.

This approach enabled the determination of the minimum illumination thresholds (lower detection limits) at which the DSSCs remain operational.

At each illumination level, the power conversion efficiencies of the devices were carefully calculated and are summarized in Tables 1-4. In the tables, (V_{OC}) and (J_{SC}) correspond to the open-circuit voltage and short-circuit current density, while P_{in} denotes the incident illumination intensity applied to the cells.

Table 1. Open Circuit Voltage Performances of the DSSCs' which combined by using TiO₂ and ZnO/TiO₂ photo electrodes

| Light Intensity (mW cm ⁻²) | V _{OC} (mV) | | | | | | |
|---|---------------------------------|---------|------|-------------------------------------|----------|------|-----|
| | TiO ₂ photoelectrode | | | ZnO/TiO ₂ photoelectrode | | | Si |
| | P.p | P,p/CdS | N719 | P.p | P,p/ CdS | N719 | |
| 100 | 608 | 620 | 646 | 618 | 624 | 656 | 486 |
| 15 | 567 | 607 | 489 | 604 | 604 | 610 | 419 |
| 8 | 570 | 548 | 477 | 570 | 580 | 583 | 388 |
| 2 | 537 | 542 | 452 | 537 | 506 | 545 | 400 |
| 1 | 504 | 488 | 437 | 504 | 483 | 520 | 340 |
| 0.5 | 470 | 444 | 422 | 470 | 415 | 446 | 310 |
| 0.2 | 437 | 388 | 407 | 437 | 362 | 390 | 276 |
| 0.1 | 391 | 208 | 391 | 404 | 194 | 209 | 244 |
| 0.05 | 376 | 150 | 376 | 370 | 170 | 157 | 242 |
| 0.01 | 361 | 138 | 361 | 337 | 130 | 118 | 210 |

The open-circuit voltage (V_{OC}) values obtained under varying light intensities provide important insight into the charge separation efficiency and recombination dynamics within the DSSC structures. As shown in Table 1, for both TiO₂ and ZnO/TiO₂-based photoelectrodes, cells sensitized with the commercial N719 dye exhibited the highest V_{OC} values under all illumination conditions, consistent with its well-established electrochemical alignment and stability. Notably, the ZnO/TiO₂ photoelectrodes consistently yielded slightly higher V_{OC} values compared to TiO₂-only counterparts, especially at high and moderate light intensities. For instance, at 100 mW/cm², N719-sensitized ZnO/TiO₂-based DSSCs reached a V_{OC} of 656 mV, compared to 646 mV for TiO₂-based ones.

However, the performance gap between TiO₂ and ZnO/TiO₂ structures narrows under extremely low-light conditions (e.g., 0.01 mW/cm²), where all devices experience a drop in V_{OC} due to reduced photoinduced carrier generation. In this regime, the natural dye (*P. pterocarpum*) and its CdS-modified variant showed a more gradual decrease in V_{OC}, suggesting more stable photovoltage generation in low-light environments. Particularly, *P. pterocarpum*-based DSSCs retained a V_{OC} of 361 mV (TiO₂) and 337 mV (ZnO/TiO₂), indicating relatively low recombination even under limited photon flux.

These results suggest that ZnO nanorod integration contributes to slightly enhanced charge separation under standard conditions, but its relative advantage diminishes under minimal illumination. Conversely, the natural dye-based configurations exhibit more stable V_{OC} behavior across a wide range of light intensities, reinforcing their suitability for indoor or diffuse light applications, where consistent voltage output is critical for reliable photodetector operation.

Table 2. Short Circuit Current Performances of the DSSCs' which combined by using TiO₂ and ZnO/TiO₂ photoelectrodes

| Light Intensity (mW cm ⁻²) | J _{SC} (mA cm ⁻²) | | | | | | Si |
|--|--|---------|-------|-------------------------------------|----------|-------|-------|
| | TiO ₂ photoelectrode | | | ZnO/TiO ₂ photoelectrode | | | |
| | P.p | P.p/CdS | N719 | P.p | P.p/ CdS | N719 | |
| 100 | 17.79 | 18.36 | 18.59 | 19.14 | 18.45 | 20.19 | 52.76 |
| 15 | 7.15 | 7.65 | 7.15 | 12.15 | 6.84 | 7.69 | 18.01 |
| 8 | 11.26 | 6.36 | 5.81 | 11.36 | 11.79 | 11.85 | 9.84 |
| 2 | 5.63 | 10.21 | 11.08 | 9.74 | 6.08 | 10.26 | 0.00 |
| 1 | 5.21 | 1.51 | 10.40 | 8.50 | 1.51 | 8.94 | 0.01 |
| 0.5 | 2.35 | 4.60 | 0.10 | 4.40 | 0.10 | 4.63 | 0.01 |
| 0.2 | 1.59 | 3.86 | 0.09 | 3.68 | 0.09 | 3.88 | 0.02 |
| 0.1 | 2.21 | 2.31 | 0.07 | 0.94 | 0.07 | 2.32 | 0.02 |
| 0.05 | 1.30 | 1.36 | 0.05 | 0.43 | 1.37 | 0.47 | 0.04 |
| 0.01 | 0.75 | 0.24 | 0.04 | 0.24 | 0.79 | 0.39 | 0.01 |

In Table 2, the short-circuit current density J_{SC} values obtained under varying illumination intensities provide further insight into the light-harvesting capability and charge injection efficiency of the DSSC structures. Under standard illumination (100 mW/cm²), DSSCs based on ZnO/TiO₂ photoanodes exhibited generally higher J_{SC} values than their TiO₂-only counterparts, particularly in the natural and N719 dye-based configurations. For instance, the J_{SC} of the *P. pterocarpum*-based cell increased from 17.79 mA/cm² (TiO₂) to 19.14 mA/cm² (ZnO/TiO₂), highlighting the role of ZnO nanorods in improving dye adsorption and facilitating electron transport due to their larger surface area and enhanced crystallinity [20, 25].

Interestingly, the CdS co-sensitized cells exhibited variable performance across light intensities. While CdS incorporation improved J_{SC} in TiO₂-based cells at mid-range illumination (e.g., 10.21 mA/cm² at 2 mW/cm²), it did not consistently enhance performance in the ZnO/TiO₂ structures, suggesting potential recombination or energy mismatch effects that may arise under certain conditions.

At ultra-low illumination levels (≤ 0.05 mW/cm²), natural dye-based DSSCs continued to exhibit measurable current output, in contrast to the rapid performance degradation of the commercial silicon device. Notably, *P. pterocarpum*-CdS/TiO₂ and CdS/ZnO/TiO₂ devices retained J_{SC} values of 1.36 mA/cm² and 1.37 mA/cm² respectively at 0.05 mW/cm², confirming their high sensitivity under weak light. The natural dye's broad absorption characteristics and slow recombination kinetics, coupled with ZnO's improved electron mobility, likely contribute to the stable photocurrent response even at minimal illumination levels.

These findings reinforce the potential of natural dye-sensitized ZnO/TiO₂ structures for low-light environments and suggest that CdS co-sensitization may offer light-intensity-dependent benefits, particularly when tuned to optimize spectral overlap and charge dynamics.

Table 3. Fill Factor Performances of the DSSCs' which are combined by using TiO₂ and ZnO/TiO₂ photoelectrodes

| Light Intensity (mW cm ⁻²) | FF | | | | | | Si |
|--|---------------------------------|---------|------|-------------------------------------|----------|------|------|
| | TiO ₂ photoelectrode | | | ZnO/TiO ₂ photoelectrode | | | |
| | P.p | P.p/CdS | N719 | P.p | P.p/ CdS | N719 | |
| 100 | 0.53 | 0.60 | 0.67 | 0.58 | 0.60 | 0.62 | 0.48 |
| 15 | 0.36 | 0.33 | 0.21 | 0.21 | 0.37 | 0.36 | 0.35 |
| 8 | 0.21 | 0.30 | 0.29 | 0.17 | 0.16 | 0.18 | 0.35 |
| 2 | 0.10 | 0.07 | 0.07 | 0.08 | 0.12 | 0.07 | 0.05 |
| 1 | 0.06 | 0.26 | 0.05 | 0.05 | 0.27 | 0.05 | 0.03 |
| 0.5 | 0.06 | 0.03 | 1.60 | 0.04 | 1.61 | 0.04 | 0.01 |
| 0.2 | 0.04 | 0.02 | 0.80 | 0.02 | 0.90 | 0.02 | 0.00 |
| 0.1 | 0.02 | 0.03 | 0.63 | 0.04 | 1.27 | 0.03 | 0.00 |
| 0.05 | 0.02 | 0.04 | 0.55 | 0.05 | 0.04 | 0.01 | 0.00 |
| 0.01 | 0.02 | 0.16 | 0.44 | 0.07 | 0.06 | 0.01 | 0.00 |

The fill factor (FF), which reflects the electrical quality and internal resistance of a solar cell, is a key determinant of overall photovoltaic efficiency. The FF data presented across varying light intensities reveal distinct trends between TiO₂ and ZnO/TiO₂ photoelectrodes. Under standard illumination (100 mW/cm²), FF values ranged from 0.53 to 0.67 for TiO₂-based DSSCs and from 0.58 to 0.62 for ZnO/TiO₂ counterparts. Notably, the commercial N719 dye consistently yielded the highest FF in both architectures, indicating its superior charge transfer kinetics and minimal series resistance.

For natural dyes, CdS co-sensitization generally improved FF, particularly under low-light conditions. For instance, at 0.01 mW/cm², the FF of P.p/CdS-based ZnO/TiO₂ DSSCs reached 0.06, compared to only 0.02 for the non-CdS variant. This suggests that CdS acts not only as a light-absorbing co-sensitizer but also as a barrier layer that reduces recombination and enhances charge selectivity, leading to better fill factor performance in photon-limited environments.

Interestingly, some irregular values—such as anomalously high FFs (e.g., 1.60 at 0.5 mW/cm² for N719)—may indicate measurement artifacts or non-ideal diode behavior under very weak illumination, possibly related to capacitive effects or unstable shunt resistance under transient conditions. These deviations warrant further investigation under controlled pulsed-light conditions to isolate transient current responses.

Overall, the ZnO/TiO₂ photoelectrodes tended to show slightly better FF retention at low illumination levels, particularly in CdS-modified structures. This observation aligns with the improved electron mobility of ZnO and its ability to maintain consistent charge transport in low-photon flux environments. The combination of natural dye, ZnO nanostructures, and CdS co-sensitization thus appears to synergistically support not only J_{SC} and V_{OC}, but also FF stability—particularly under challenging light conditions relevant to indoor and low-light photodetector applications.

Table 4. Power Conversion Efficiency Performances of the DSSCs' which are combined by using TiO₂ and ZnO/TiO₂ photo electrodes

| Light Intensity (mW cm ⁻²) | μ (%) | | | | | | Si |
|--|---------------------------------|---------|-------|-------------------------------------|----------|-------|--------|
| | TiO ₂ photoelectrode | | | ZnO/TiO ₂ photoelectrode | | | |
| | P.p | P.p/CdS | N719 | P.p | P.p/ CdS | N719 | |
| 100 | 5.78 | 6.87 | 8.06 | 6.84 | 6.92 | 8.15 | 3.80 |
| 15 | 8.49 | 9.08 | 9.09 | 8.67 | 9.09 | 10.05 | 1.56 |
| 8 | 9.57 | 10.44 | 11.18 | 10.39 | 10.88 | 12.35 | 1.32 |
| 2 | 10.35 | 13.16 | 12.44 | 11.99 | 12.44 | 13.26 | 0.0003 |
| 1 | 10.73 | 12.69 | 13.11 | 12.63 | 13.18 | 14.49 | 0.0005 |
| 0.5 | 12.32 | 13.86 | 13.92 | 13.85 | 13.92 | 15.3 | 0.0008 |
| 0.2 | 13.80 | 14.62 | 14.62 | 14.46 | 14.62 | 15.98 | 0.0010 |
| 0.1 | 15.05 | 16.29 | 16.34 | 15.96 | 16.34 | 16.64 | 0.0013 |
| 0.05 | 16.29 | 17.88 | 19.40 | 16.69 | 18.01 | 19.49 | 0.0023 |
| 0.01 | 17.22 | 18.51 | 20.51 | 18.51 | 19.04 | 20.61 | 0.0008 |

The power conversion efficiency (PCE, η) data obtained from the DSSC configurations provide a comprehensive assessment of their overall performance under varying illumination conditions. As shown in Figure 4, under standard sunlight (100 mW/cm²), the highest efficiencies were achieved by DSSCs sensitized with the commercial N719 dye, reaching 8.06% with TiO₂ and 8.15% with ZnO/TiO₂ photoanodes. These values align with N719's well-established characteristics of efficient charge injection and photostability. Among the natural dye-based systems, *P. pterocarpum* + CdS co-sensitized cells consistently outperformed their non-CdS counterparts, achieving up to 6.92% efficiency with the ZnO/TiO₂ structure. This improvement highlights the beneficial effect of CdS in expanding the absorption spectrum and enhancing electron injection through favorable band alignment.

Remarkably, all DSSC configurations remained operational even under extremely low illumination (0.01 mW/cm²), emphasizing their high sensitivity and photodetection potential. At this lowest intensity level, the N719-based cells again demonstrated the highest PCE, reaching 20.61% (ZnO/TiO₂) and 20.51% (TiO₂). However, the CdS-enhanced natural dye cells followed closely, with 19.04% (ZnO/TiO₂) and 18.51% (TiO₂). Even the DSSCs sensitized with unmodified *P. pterocarpum* dye exhibited competitive efficiencies of 18.51% (ZnO/TiO₂) and 17.22% (TiO₂), revealing strong potential in low-light conditions. These values significantly exceeded the performance of the commercial c-Si photodetector, which dropped below 0.001% under the same conditions.

This trend suggests that the inherently slower recombination kinetics and possible trap-assisted charge retention mechanisms in natural dye systems may confer an advantage under ultra-low light conditions—where conventional silicon-based photovoltaics typically fail. Furthermore, ZnO nanorods, by increasing the effective surface area and facilitating efficient electron transport, further enhance this performance.

These findings underscore the dual functionality of natural dye-sensitized DSSCs—particularly those integrated with ZnO nanostructures and CdS co-sensitizers—as both effective solar energy harvesters and high-sensitivity optical detectors. While synthetic dyes like N719 continue to dominate under standard illumination, natural dye-based DSSCs demonstrate exceptional promise in ambient and indoor lighting scenarios. Their ability to outperform commercial c-Si devices under dim light, combined with their low cost and eco-friendly nature, strongly supports their integration into sustainable, versatile optoelectronic technologies.

Figure 3 illustrates the current–voltage (I–V) characteristics of the fabricated cells, and the performance parameters extracted from these curves are summarized in Tables 1-4.

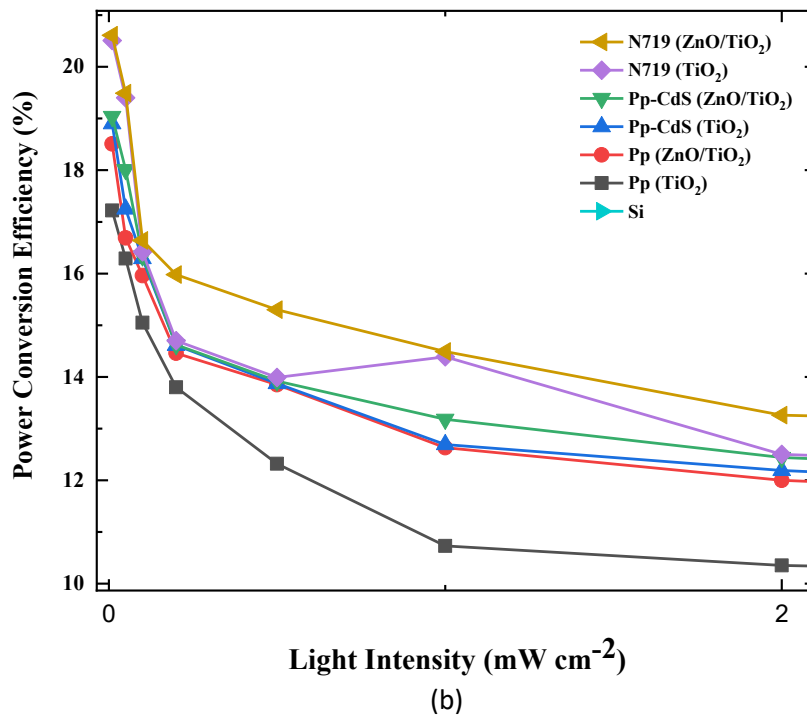
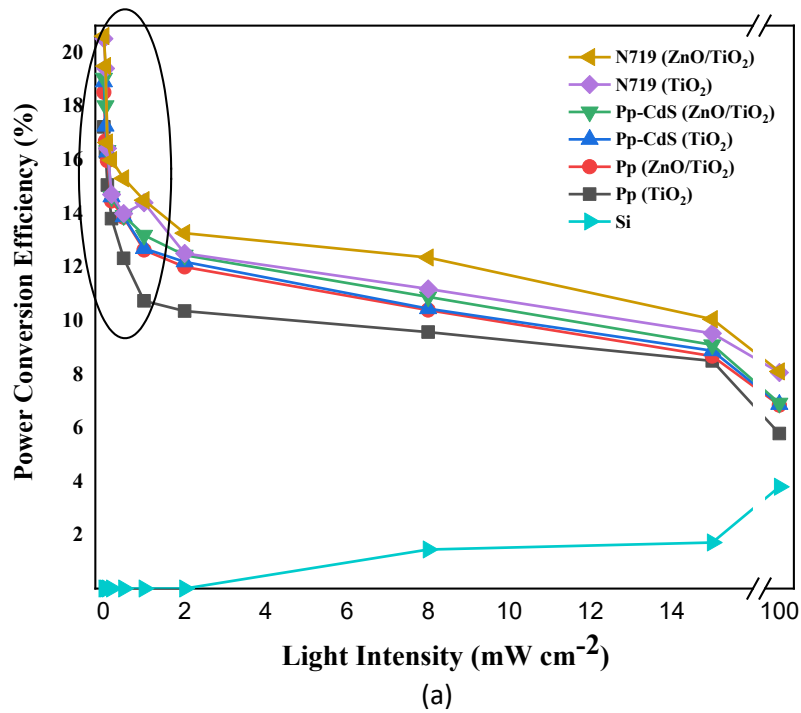


Figure 3. Power Conversion Efficiencies of the DSSCs and c-Si sensor, based on the various light intensities that range as (a) 100, 15, 8, 2, 1, 0.5, 0.2, 0.1, 0.05, and 0.01 mW/cm² respectively, (b) measurements in the 2 mW/cm² and lower illumination levels

Figure 3 clearly reveals that the DSSCs fabricated with natural dyes also demonstrated remarkable performance under low-light conditions. These results strongly suggest that natural dyes such as *P. pterocarpum* possess excellent photodetector sensitivity, particularly when enhanced by ZnO nanorods and CdS co-sensitization. The incorporation of ZnO nanostructures not only increased the surface area for dye adsorption but also improved electron transport and reduced recombination, leading to an enhanced energy conversion efficiency of up to 6.84% under standard light conditions. CdS further elevated the efficiency from 5.8% to 6.9%, while also improving key photovoltaic parameters such as

short-circuit current density (J_{sc}) and open-circuit voltage (V_{oc}), which is in line with findings reported in similar studies [15–19].

The improvement in device performance with CdS co-sensitization can be attributed to its favorable bandgap alignment and complementary light absorption properties. CdS, a II–VI semiconductor with a direct bandgap of approximately 2.4 eV, extends the photoresponse of the DSSC toward the visible region, enhancing overall light harvesting. When used in conjunction with a natural dye such as *P. pterocarpum*, CdS can act as an additional sensitizer that absorbs shorter-wavelength photons, while the organic dye covers longer wavelengths. This complementary absorption broadens the effective spectral response of the device. Furthermore, the conduction band of CdS is positioned higher than that of TiO₂, facilitating efficient electron injection into the photoanode and reducing charge recombination at the dye–electrolyte interface. Such synergistic band alignment improves charge separation and transport, which ultimately contributes to the observed gains in power conversion efficiency.

The comparative analysis also highlights that DSSCs significantly outperformed commercial c-Si photodetectors under low light, offering nearly ten times higher output power and fill factor. This makes them particularly advantageous in scenarios with limited illumination—such as early morning, late evening, indoor lighting, or overcast conditions.

In summary, this study presents a comprehensive investigation into the use of a natural dye extracted from *P. pterocarpum* in DSSC applications involving TiO₂ and ZnO nanostructured photoelectrodes. The findings confirm that natural dyes are not only renewable and eco-friendly but also highly effective under low-light, making them suitable for next-generation photovoltaic and photodetector technologies. The integration of ZnO nanorods and CdS co-sensitizers further enhances device performance, paving the way for cost-effective, sustainable, and high-sensitivity optoelectronic systems. Future research may focus on improving the chemical stability and long-term durability of natural dyes to ensure their scalability and industrial applicability.

IV. CONCLUSION

This study demonstrates the potential of natural dye-based dye-sensitized solar cells (DSSCs), enhanced with CdS co-sensitization and ZnO nanorod-integrated TiO₂ photoelectrodes, for dual functionalities: solar energy harvesting and low-light photodetection. The synergistic combination of *Peltophorum pterocarpum* dye, CdS nanoparticles, and ZnO nanostructures significantly improved charge transfer and light absorption while reducing recombination losses—particularly benefiting the natural dye systems. As a result, these DSSCs achieved competitive efficiencies under standard illumination and outstanding performance under ultra-low light conditions (>18%).

While the commercial N719-based DSSCs recorded the highest efficiency (8.15%) under standard light (100 mW/cm²), the natural dye-based configurations reached up to 6.92%, indicating their viability as cost-effective alternatives. More notably, under ultra-low light (0.01 mW/cm²), the natural dye-based DSSCs maintained measurable output and outperformed conventional c-Si photodetectors, emphasizing their potential in ambient light sensing and indoor photovoltaic applications.

Overall, this research bridges green material utilization with nanostructural engineering, contributing to the development of next-generation, eco-friendly, and multifunctional optoelectronic devices. Future work should focus on enhancing the long-term chemical stability of natural dyes, optimizing electrolyte compatibility, and validating device performance under real-world and scalable operational conditions.

Article Information

Acknowledgments: This work was supported by TÜBİTAK under Project No. 124M760, titled “Boyayla Duyarlılaştırılmış Güneş Pilleri İçin Arka Elektrot Olarak Pt Nanoparçacık Katkılı Grafitik Karbon Nitrür (g-C₃N₄)/Polianilin Nanokompozit Kullanılmasıyla Korozyonun Azaltılması ve Güneş Pili Ömrünün ve Performansının Arttırılması Üzerine Deneysel Bir Çalışma”.

The author would also like to express her sincere thanks to the editor and anonymous reviewers for their valuable comments and suggestions.

Author’s Contributions: Writing—original draft, review, analysis, and editing were performed solely by Mücella ÖZBAY KARAKUŞ. The author has read and approved the final version of the manuscript.

Artificial Intelligence Statement: No any Artificial Intelligence tool is used in this paper.

Conflict of Interest Disclosure: No potential conflict of interest was declared by authors.

Plagiarism Statement: This article was scanned by the plagiarism program.

V. REFERENCES

- [1] H. Abdullah, N. H. Yunos, S. Mahalingam, M. Ahmad and B. Yulianto, “Photovoltaic and EIS performance of SnO₂/SWCNTS based–sensitized solar cell,” *Procedia Engineering*, vol. 170, pp. 1–7, 2017.
- [2] H. Hafez, M. Saif and M. S. A. Abdel-Mottaleb, “Down-converting lanthanide doped TiO₂ photoelectrodes for efficiency enhancement of dye-sensitized solar cells,” *Journal of Power Sources*, vol. 196, no. 13, pp. 5792–5796, 2011.
- [3] M. I. Hoffert et al., “Energy implications of future stabilization of atmospheric CO₂ content,” *Nature*, vol. 395, no. 6705, pp. 881–884, 1998.
- [4] J. Zhao, A. Wang and M. A. Green, “24.5% Efficiency silicon PERT cells on MCZ substrates and 24.7% efficiency PERL cells on FZ substrates,” *Progress in Photovoltaics: Research and Applications*, vol. 7, no. 6, pp. 471–474, 1999.
- [5] S. Mathew et al., “Dye-sensitized solar cells with 13% efficiency achieved through the molecular engineering of porphyrin sensitizers,” *Nature chemistry*, vol. 6, no. 3, pp. 242–247, 2014.
- [6] M. A. M. Al-Alwani, N. A. Ludin, A. B. Mohamad, A. A. H. Kadhum and K. Sopian, “Extraction, preparation and application of pigments from *Cordyline fruticosa* and *Hylocereus polyrhizus* as sensitizers for dye-sensitized solar cells,” *Spectrochimica Acta Part A: Molecular and Biomolecular Spectroscopy*, vol. 179, pp. 23–31, 2017.
- [7] B. E. Hardin, H. J. Snaith and M. D. McGehee, “The renaissance of dye-sensitized solar cells,” *Nature Photonics*, vol. 6, no. 3, pp. 162–169, 2012.
- [8] T. M. El-Agez, A. A. El Tayyan, A. Al-Kahlout, S. A. Taya and M. S. Abdel-Latif, “Dye-sensitized solar cells based on ZnO films and natural dyes,” *International Journal of Materials and Chemistry*, vol. 2, no. 3, pp. 105–110, 2012.

- [9] S. Shalini, R. Balasundaraprabhu, T. S. Kumar, K. Sivakumaran and M. D. Kannan, "Synergistic effect of sodium and yeast in improving the efficiency of DSSC sensitized with extract from petals of *Kigelia africana*," *Optical Materials*, vol. 79, pp. 210–219, 2018.
- [10] H. Chang and Y. J. Lo, "Pomegranate leaves and mulberry fruit as natural sensitizers for dye-sensitized solar cells," *Solar Energy*, vol. 84, no. 10, pp. 1833–1837, 2010.
- [11] H. Chang, H. M. Wu, T. L. Chen, K. D. Huang, C. S. Jwo and Y. J. Lo, "Dye-sensitized solar cell using natural dyes extracted from spinach and ipomoea," *Journal of Alloys and Compounds*, vol. 495, no. 2, pp. 606–610, 2010.
- [12] Q. L. Ma, S. Ma and Y. M. Huang, "Enhanced photovoltaic performance of dye-sensitized solar cell with ZnO nanohoneycombs decorated TiO₂ photoanode," *Materials letters*, vol. 218, pp. 237–240, 2018.
- [13] D. Sinha, D. De and A. Ayaz, "Performance and stability analysis of curcumin dye as a photosensitizer used in nanostructured ZnO based DSSC," *Spectrochimica Acta Part A: Molecular and Biomolecular Spectroscopy*, vol. 193, pp. 467–474, 2018.
- [14] S. Yadav and A. Tadinada, "Enhanced patient care through collaborative team play: An orthodontist and an OMF radiologist's collective perspective," *APOS Trends in Orthodontics*, vol. 5, no. 3, pp. 94, 2015.
- [15] S. Ren, L. Y. Chang, S. K. Lim, J. Zhao, M. Smith, N. Zhao and S. Gradečak, "Inorganic–organic hybrid solar cell: Bridging quantum dots to conjugated polymer nanowires," *Nano letters*, vol. 11, no. 9, pp. 3998–4002, 2011.
- [16] H. O. Shoyiga, S. O. Akpasi, J. Akpan, U. O. Amune and S. L. Kiambi, "Novel photoactive material and fabrication techniques for solar cells application: Nanocellulose-based graphene oxide CdS composite," *Clean Energy*, vol. 8, no. 2, pp. 189–216, 2024.
- [17] H. C. Liao, S. Y. Chen and D. M. Liu, "In-situ growing CdS single-crystal nanorods via P3HT polymer as a soft template for enhancing photovoltaic performance," *Macromolecules*, vol. 42, no. 17, pp. 6558–6563, 2009.
- [18] S. Sagadevan and K. Pandurangan, "Synthesis, structural, optical and electrical properties of cadmium sulphide thin films by chemical bath deposition method," *International Journal of ChemTech Research*, vol. 6, pp. 3748–3752, 2014.
- [19] A. Triyanto, N. Ali and H. Salleh, "Development of natural dye photosensitizers for dye-sensitized solar cells: A review," *Environmental Science and Pollution Research*, vol. 31, pp. 31679–31690, 2024.
- [20] V. Cauda et al., "Multi-functional energy conversion and storage electrodes using flower-like zinc oxide nanostructures," *Energy*, vol. 65, pp. 639–646, 2014.
- [21] N. Memarian, I. Concina, A. Braga, S. M. Rozati, A. Vomiero and G. Sberveglieri, "Hierarchically assembled ZnO nanocrystallites for high-efficiency dye-sensitized solar cells," *Angewandte Chemie-International Edition*, vol. 50, no. 51, p. 12321, 2011.
- [22] P. Dhamodharan, C. Manoharan, S. Dhanapandian and P. Venkatachalam, "Dye-sensitized solar cell using sprayed ZnO nanocrystalline thin films on ITO as photoanode," *Spectrochimica Acta Part A: Molecular and Biomolecular Spectroscopy*, vol. 136, pp. 1671–1678, 2015.

- [23] L. De Marco et al., "Single crystal mesoporous ZnO platelets as efficient photoanodes for sensitized solar cells," *Solar Energy Materials and Solar Cells*, vol. 168, pp. 227–233, 2017.
- [24] D. Y. Son, K. H. Bae, H. S. Kim and N. G. Park, "Effects of seed layer on growth of ZnO nanorod and performance of perovskite solar cell," *The Journal of Physical Chemistry C*, vol. 119, no. 19, pp. 10321–10328, 2015.
- [25] J. A. Anta, E. Guillén and R. Tena-Zaera, "ZnO-based dye-sensitized solar cells," *The Journal of Physical Chemistry C*, vol. 116, no. 21, pp. 11413–11425, 2012.
- [26] L. Nasi et al., "Mesoporous single-crystal ZnO nanobelts: supported preparation and patterning," *Nanoscale*, vol. 5, no. 3, pp. 1060–1066, 2013.
- [27] M. Grätzel, "Photovoltaic performance and long-term stability of dye-sensitized mesoscopic solar cells," *Comptes Rendus Chimie*, vol. 9, no. 5–6, pp. 578–583, 2006.
- [28] R. Sasikumar, T. W. Chen, S. M. Chen, S. P. Rwei and S. K. Ramaraj, "Developing the photovoltaic performance of dye-sensitized solar cells (DSSCs) using a SnO₂-doped graphene oxide hybrid nanocomposite as a photo-anode," *Optical Materials*, vol. 79, pp. 345–352, 2018.
- [29] P. Sanjay, K. Deepa, J. Madhavan and S. Senthil, "Optical, spectral and photovoltaic characterization of natural dyes extracted from leaves of *Peltophorum pterocarpum* and *Acalypha amentacea* used as sensitizers for ZnO-based dye-sensitized solar cells," *Optical Materials*, vol. 83, pp. 192–199, 2018.
- [30] G. Bardizza, D. Pavanello, R. Galleano, T. Sample and H. Müllejans, "Calibration procedure for solar cells exhibiting slow response and application to a dye-sensitized photovoltaic device," *Solar Energy Materials and Solar Cells*, vol. 160, pp. 418–424, 2017.
- [31] A. M. El-Zohry and B. Zietz, "Electron dynamics in dye-sensitized solar cells influenced by dye–electrolyte complexation," *The Journal of Physical Chemistry C*, vol. 124, no. 30, pp. 16300–16307, 2020.
- [32] M. Ö. Karakuş, M. E. Yakışıklar, A. Delibaş, E. Ayyıldız and H. Çetin, "Anionic and cationic polymer-based quasi-solid-state dye-sensitized solar cell with poly(aniline) counter electrode," *Solar Energy*, vol. 195, pp. 565–572, 2020.